CERM

Retinoic acid loaded with chitosan nanoparticles improves spermatogenesis in scrotal hyperthermia in mice

Fatemeh Mazini[1], Mohammad-Amin Abdollahifar[2,3], Hassan Niknejad[4], Asma Manzari-Tavakoli[5], Mohsen Zhaleh[1], Reza Asadi-Golshan[6], Ali Ghanbari[1]

[1]Department of Anatomical Science, Kermanshah University of Medical Sciences, Kermanshah; [2]Urogenital Stem Cell Research Center, Shahid Beheshti University of Medical Sciences, Tehran; Departments of [3]Biology and Anatomical Sciences, [4]Pharmacology, School of Medicine, Shahid Beheshti University of Medical Sciences, Tehran; [5]ATMP Department, Breast Cancer Research Center, Motamed Cancer Institute, ACECR, Tehran; [6]Department of Anatomy, School of Medicine, Tehran University of Medical Sciences, Tehran, Iran

Objective: High temperatures can trigger cellular oxidative stress and disrupt spermatogenesis, potentially leading to male infertility. We investigated the effects of retinoic acid (RA), chitosan nanoparticles (CHNPs), and retinoic acid loaded with chitosan nanoparticles (RACHNPs) on spermatogenesis in mice induced by scrotal hyperthermia (Hyp).

Methods: Thirty mice (weighing 25 to 30 g) were divided into five experimental groups of six mice each. The groups were as follows: control, Hyp induced by a water bath (43 °C for 30 minutes/day for 5 weeks), Hyp+RA (2 mg/kg/day), Hyp+CHNPs (2 mg/kg/72 hours), and Hyp+RACHNPs (4 mg/kg/72 hours). The mice were treated for 35 days. After the experimental treatments, the animals were euthanized. Sperm samples were collected for analysis of sperm parameters, and blood serum was isolated for testosterone measurement. Testis samples were also collected for histopathology assessment, reactive oxygen species (ROS) evaluation, and RNA extraction, which was done to compare the expression levels of the *bax*, *bcl2*, *p53*, *Fas*, and *FasL* genes among groups. Additionally, immunohistochemical staining was performed.

Results: Treatment with RACHNPs significantly increased stereological parameters such as testicular volume, seminiferous tubule length, and testicular cell count. Additionally, it increased testosterone concentration and improved sperm parameters. We observed significant decreases in ROS production and caspase-3 immunostaining in the RACHNP group. Moreover, the expression levels of *bax*, *p53*, *Fas*, and *FasL* significantly decreased in the groups treated with RACHNPs and RA.

Conclusion: RACHNPs can be considered a potent antioxidative and antiapoptotic agent for therapeutic strategies in reproductive and regenerative medicine.

Keywords: Azoospermia; Chitosan; Hyperthermia; Nanoparticles; Retinoic acid; Scrotum; Spermatogenesis

Introduction

Spermatogenesis and fertility require a testicular temperature that is approximately 2 to 4 °C below the core body temperature [1], as research has demonstrated that scrotal hyperthermia (Hyp) can harm sperm and testicular germ cells [2]. Several lifestyle factors, including clothing [3], laptop use [4], microwave oven exposure [5], mobile phone use [6], clinical diseases such as cryptorchidism and varicocele [7,8], and occupational hazards can disrupt testicular temperature [3]. Elevated testicular temperature can result in a signifi-

F Mazini et al. Retinoic acid loaded chitosan nanoparticles improve spermatogenesis

CERM

cant but reversible decrease in spermatogenesis and total sperm count, potentially leading to azoospermia. This is due to an increased loss of germ cells, reduced expression of proliferating cell nuclear antigen, and an imbalance between oxidative stress and antioxidant capacity [9-11]. Various treatments aimed at enhancing spermatogenesis have been investigated, including the use of vitamin C and/or vitamin E along with other antioxidants. These treatments have demonstrated promising results in improving semen quality [12,13].

Retinoic acid (RA), a derivative of vitamin A, is instrumental in regulating cell proliferation and differentiation in the development of organs such as the eye, heart, pancreas, and testis. RA is required for signaling and transcriptional control during both male and female development. It interacts with receptor proteins that influence the transcription of several genes vital for these processes [14,15]. A diet deficient in vitamin A can induce infertility in feeding rats, resulting in the inability to produce viable sperm; this underscores the importance of RA in spermatogenesis. However, the administration of exogenous RA can restore spermatogenesis in these animals [16]. The importance of substances such as RA has been proposed for many spermatogenic processes, including the differentiation of spermatogonia [17], the establishment of the blood-testis barrier, and the release of mature spermatids into the lumen [18,19].

Vitamin A is a hydrophobic compound that can easily become inactive or rapidly degrade in aqueous systems. It is poorly soluble in water and has low stability in the presence of oxidants, light, heat, temperature, and moisture. These factors limit its clinical application. However, the stability and dispersibility of vitamin A can be increased by incorporating it into a carrier with beneficial physical and chemical properties [20]. Recent advancements in nanotechnology have broadened the potential medical applications of such carriers [21,22]. Nanoparticles (NPs) have biological effects that may enhance male fertility by improving the quality of sperm cells *in vivo* or *in vitro*. However, the effects of NPs at the cellular and tissue levels are not fully understood [23]. Chitosan, a derivative of chitin, is the second most abundant biomass on earth. It has been used as a delivery system for proteins, nutraceuticals, genes, growth factors, and drugs due to its low toxicity, biocompatibility, biodegradability, mucoadhesion, and low production cost [24-26]. Chitosan nanoparticles (CHNPs), which are positively charged at low pH levels, can form polyelectrolytes in solution by associating with anions [27]. CHNPs containing RA may positively impact sperm parameters and testicular tissue characteristics. In the current study, we investigated the use of retinoic acid loaded with chitosan nanoparticles (RACHNPs), an effective technique for the slow release of vitamin A, to promote the proliferation and differentiation of spermatogonia and sperm parameters in mice subjected to Hyp.

Methods

1. Synthesis and characterization of CHNPs

The CHNPs were synthesized using a method similar to the process detailed in our prior research [28]. In brief, 0.9 mg/mL of medium-molecular-weight chitosan (50,000 to 190,000, Sigma-Aldrich) was mixed into 5 mL of 0.5% acetic acid. This mixture underwent continuous magnetic stirring at room temperature for 24 hours. The pH of the chitosan solution was adjusted to 5.5 using a 2 M NaOH solution. Separately, polyanion sodium tripolyphosphate (TPP) (Sigma-Aldrich) was dissolved in deionized water to attain a final concentration of 0.25 mg/mL. Then, 2 mL of TPP solution was added to the chitosan solution at a rate of 0.2 mL/min while stirring the mixture for 1 hour to form CHNPs. These CHNPs were obtained after freeze-drying for 24 hours. The average particle size was determined using dynamic light scattering (SZ-100Z; HORIBA Jobin Yvon), and the surface charge of the NPs was measured with a zeta potential analyzer (HORIBA Jobin Yvon).

2. Preparation of RACHNPs

Initially, 25 mg of CHNP powder was dispersed in a 5-mL mixture of deionized water and alcohol in equal proportions. Separately, RA was dissolved to a concentration of 20 mg/mL in dimethyl formamide (DMF). This solution was then added dropwise to the pre-prepared CHNP suspension (5 mL) under the action of a magnetic stirrer operating at 150 rpm. This was done for 1 hour at room temperature in a dark environment. The resulting solution was then placed on a shaker for 24 hours. Subsequently, drug loaded NPs were dialyzed using a dialysis membrane with a cut-off value of 12 to 14 kDa (D9402; Sigma-Aldrich), to completely remove non-reactive and oxidant substances. The dialyzed sample was centrifuged at 10,000 rpm for 1 hour, and the resulting precipitate was placed in a freeze dryer to dry for 24 hours. The powder obtained was used to perform Fourier-transform infrared spectroscopy (FTIR) testing, to calculate the amount of drug loaded into the CHNPs, and to assess drug release.

To quantify the loaded drug, a specific weight of RACHNPs was dissolved in 1 mL of DMF and agitated on a shaker. The mixture was then centrifuged at 4,000 rpm for 5 minutes, and the optical absorption of the supernatant was measured using a spectrophotometer (BioTek Synergy HTX; Agilent Technologies Inc.). For this study, a standard curve for RA was established by preparing a series of RA concentrations in DMF, measured at a wavelength of 352 nm. The loading capacity (LC %) was then calculated using the equation derived from the standard curve:

Equation 1. LC% = Wf/Wn × 100

(Wn = weight of NPs; Wf = concentration of loaded retinoic acid in the NPs)

3. Fourier-transform infrared spectroscopy

The chemical structures of RA, CHNPs, and RACHNPs were analyzed using FTIR in the wavenumber range of 4,000 to 400 cm^{-1} resolution (Thermo-Avatar; Thermo Fisher Scientific).

4. Examination of RA release from CHNPs

The drug release investigation was adapted from previous research [29]. To evaluate the release of RA from the RACHNPs, 2.5 mg of RACHNPs was incubated in 500 μL of phosphate-buffered saline (PBS; pH = 7.4) at 37 °C. The suspension was then centrifuged at 10,000 rpm for 30 minutes at regular intervals of 2, 4, 6, 8, 12, 16, 20, 24, 36, 48, 60, 72, 84, 96, 108, and 120 hours. At specific time points, a 400-μL sample of PBS solution was collected and its absorbance measured using a spectrophotometer (BioTek Synergy HTX) at 352 nm. After each measurement, the sample was replaced with fresh PBS. Finally, the cumulative percentage of RA released from the CHNPs at different time intervals was calculated, using the equation derived from the standard curve.

5. Animal study

This study adhered to the guidelines and regulations established by the Ethics Committee of Kermanshah University of Medical Sciences (IR.KUMS.AEC.1400.024). Thirty healthy adult male Naval Medical Research Institute mice, weighing 25 to 30 g, were selected and housed under standard laboratory conditions. The animals were randomly assigned to five groups of six mice each. The first group served as the control, while the second (Hyp) was exposed to Hyp without any treatment. A third group (the RA group) received an intraperitoneal (IP) injection of RA (2 mg/kg), as per previous studies [30], following 35 days of Hyp. A fourth (the CHNP group) received an IP injection of CHNPs (2.5 mg/kg/72 h) after 35 days of Hyp. Finally, the RACHNP group received an IP injection of RACHNPs (2 mg/kg/72 hours) after 35 days of Hyp.

6. Hyperthermia induction

The animals underwent 30-minute heat shocks for 35 days. Before the daily induction of hyperthermia, each animal was anesthetized using IP injections of ketamine (100 mg/kg) and xylazine (5 mg/kg). Its scrotum and hind legs were then immersed in a water bath maintained at 43 °C [31].

7. Semen analysis

After a 70-day hyperthermia induction period, sperm samples were collected from the epididymal tail 24 hours after administration of NPs and RA. These samples were then transferred to 1 mL of Ham's F-10 medium (Product No. N6635; Sigma-Aldrich) and incubated for 20 minutes at 37 °C. Subsequently, 10 μL of the sample was placed on a slide, and sperm motility was examined under an inverted microscope. The sperm count was then determined by counting the chambers of the hemocytometer. For viability and morphology analyses, the sperm smear was placed on a slide, air-dried at room temperature, fixed in methyl alcohol, and stained with eosin-nigrosin.

8. Serum testosterone measurement

With the animals under general anesthesia, blood samples were collected from the heart. These samples were then centrifuged at 6,000 ×g for 5 minutes at 4 °C before being stored at −80 °C for future use. We measured the serum levels of testosterone in the mice using a mouse-specific enzyme-linked immunosorbent assay kit (catalog no. CSB- E11162r).

9. Tissue preparation

Before the final phase of the experiment, the animals were given a lethal dose of xylazine hydrochloride and ketamine to induce anesthesia. Tissue samples were collected from the testes and preserved in Bouin solution for 48 hours. Next, the samples were fixed in a tissue processor and subsequently embedded in paraffin. Stereological methods were employed to cut serial sections (5 μm thick for volume estimation and 25 μm thick for number estimation) using a microtome (Leica RM2125 RTS; Leica Biosystems). Each sample consisted of 10 parts between 1 and 10 randomly selected using the systematic uniform random sampling method. Hematoxylin and eosin staining (Sigma) was utilized. Notably, morphological distinctions were used to identify the cells of the testis. Leydig cells, which are polyhedral and have a round nucleus and eosinophilic cytoplasm, can be found in the interstitial tissue between seminiferous tubules. Sertoli cells, which are rare and large, may be located toward the base of the epithelium. Dome-shaped spermatogonia can be found at the epithelial basement membrane, and their nuclei may be either dark or bright. Primary spermatocytes, the largest cells of the seminiferous epithelium, can be found in the germinal epithelium. Round spermatids are visible towards the lumen.

10. Total volumes of the testis

The total testicular volume (in mm^3) was determined using equation 2, and a projection microscope was developed at the Stereology Research Center according to the Cavalieri principle.

Equation 2. V = ∑P × a/p × t

F Mazini et al.   Retinoic acid loaded chitosan nanoparticles improve spermatogenesis

CERM

ΣP represents the total number of points counted. The quantity a/p denotes the probe point area divided by the magnification factor, while t indicates the tissue section separation (or thickness of sections) [32,33].

11. Length and density of seminiferous tubules

The length and density of the seminiferous tubules were estimated using the following formula:

Equation 3. $Lv = (2\Sigma Q)/(\Sigma p \times a/f)$

where ΣQ represents the total number of seminiferous tubules, ΣP denotes the total number of points superimposed on the testis tissue, and a/f indicates the area per frame. The total length of the seminiferous tubules was estimated by multiplying the length density (Lv) by the total volume of the testis [32,33].

12. Number of testicular cells

An unbiased counting frame and an optical dissecting technique were used to determine the total number of testicular cells. Each image of a testis segment was overlaid with a neutral counting frame. We mounted a microcator (Heidenhain) on the microscope stage to take z-axis measurements. The height of the dissector was defined as the thickness of the section, subtracting 20% from both the top and bottom. The distinct morphology of the testicular cells aided in their identification. Leydig cells, which can be found in the interstitial tissue, are polyhedral and possess eosinophilic cytoplasm. The Sertoli cells of the seminiferous tubule have a small, oval, pale nucleus located at their base. Spermatogonia are dome-shaped cells with either dark or light, spherical nuclei, situated at the base of the seminiferous epithelium. Primary spermatocytes, the largest cells of the seminiferous epithelium, are found in the center of the germinal epithelium. Spermatids have a rounded appearance on the luminal side. We used equation 4 to estimate the density of testicular cells (Nv).

Equation 4. $Nv = [\Sigma Q/(\Sigma P \times a/f \times h) \times t/BA]$

where h represents the height of the dissector, t denotes the actual section thickness measured with the micrometer (here, approximately 20 μm), BA indicates the tissue section thickness as determined by cutting the sections at 25 μm, ΣQ denotes the number of counted cells, a/f indicates the area per frame, and ΣP represents the number of counting frames for all the fields. The total testicular cell count was calculated using equation 5:

Equation 5. $N_{(total)} = Nv \times V_{(final)}$

where Nv represents the testicular cell density and V denotes the testicular volume.

13. Measurement of reactive oxygen species

We utilized a modified fluorometric technique to measure reactive oxygen species (ROS) in the testis, with 2',7'-dichlorofluorescein diacetate (DCFH-DA; Sigma-Aldrich) serving as both a ROS and a cellular marker of oxidative stress. Specifically, 50 mg of testis tissue was homogenized in 600 μL of 0.1 M PBS (pH 7.4) and pre-incubated with DCFH-DA (20 μM) at 37 °C. This process allowed the probe to integrate into membrane-bound vesicles and facilitated the cleavage of the diacetate group by esterases. The conversion of DCFH into the fluorescent product 2',7'-dichlorofluorescein (DCF) was recorded using a DTX 880 multimodal detector fluorescent spectrophotometer (Beckman Coulter). This was done with excitation at 485 nm and emission at 535 nm after a 30-minute incubation period. Protein concentrations were measured following sample collection from each well, and data were reported as the percentage of the maximum fluorescence.

14. Immunohistochemical staining

The testicular tissues were first fixed, then embedded in paraffin wax. These tissues were sectioned using a microtome to a thickness of 5 μm. The tissue slices were subsequently deparaffinized and rinsed with xylene to remove the paraffin. They were then dehydrated through a series of graded ethanol baths to displace the water, effectively rehydrating them in an alcohol gradient. Blocks of 10% hydrogen peroxide were placed over the sections and incubated for 10 minutes in darkness. The sections were then incubated with the primary antibody against caspase-3 (catalog number CPP324-1-18, dilution 1:100) for 50 minutes at room temperature. The slides were further incubated with horseradish peroxidase-conjugated anti-rabbit immunoglobulin G for 40 minutes at room temperature. After this, diaminobenzidine tetrahydrochloride chromogen was added for 10 minutes, and the slides were washed three times in buffer. The final step involved counterstaining with hematoxylin for nuclear staining.

15. Quantitative real-time PCR findings

In this experiment, total RNA was isolated from mouse testicles using a high-purity RNA isolation kit (Invitrogen). After collection, the RNA samples were treated with DNase I enzyme. Next, the total purity of the extracted RNA was determined using a NanoDrop spectrophotometer (ND-1000; Thermo Scientific), measuring absorbance at 260 and 280 nm. Complementary DNA (cDNA) was synthesized with a cDNA synthesis kit (Invitrogen) according to the manufacturer's instructions. To quantify relative gene expression, quantitative re-

al-time polymerase chain reaction (qRT-PCR; TaqMan) was utilized with the QuantiTect SYBR green master mix no. RUX RT-PCR kit (21H0601).

Primers for *bax*, *bcl2*, *p53*, *FAS*, and *FasL* were designed using Oligo 6 software (Molecular Biology Insights Inc.) and are shown in Table 1. Subsequently, the efficacy of these PCR primers was evaluated using the Primer-Blast tool from the National Center for Biotechnology Information, which can be accessed at www.ncbi.nlm.nih.gov/tools/primer-blast (Table 1).

16. Statistical analysis

Statistical analysis was performed using SPSS version 17.0 (SPSS Inc.). The data are displayed as the mean ± standard error (SE). To analyze the data, we used one-way analysis of variance and the Tukey *post hoc* test for multiple comparisons. A *p*-value of less than 0.05 was considered to indicate statistical significance.

Results

1. Synthesis and characterization of CHNPs and RACHNPs: size and zeta potential

CHNPs were produced using the ionic gelation method. The formation of CHNPs occurred through electrostatic interaction between the positively charged amine groups in chitosan and the negatively charged sodium TPP. Table 2 presents the dynamic light scattering results indicating the sizes of the purified CHNPs and RACHNPs. The mean size of the CHNPs was 228.20 ± 22.78 nm, while the RACHNPs had a mean size of 324 ± 29.9 nm. Consequently, the NPs synthesized in this study can be considered suitable as a nanocarrier for RA delivery. The zeta potentials of the CHNPs and RACHNPs were found to be 32.65 and 10.8 MV, respectively.

2. Fourier-transform infrared spectroscopy

To determine the chemical structures of RA, CHNPs, and RACHNPs, we generated FTIR spectra, as depicted in Figure 1A. The FTIR absorption spectrum of chitosan revealed the peaks of the amine and carbonyl groups of the O=C-NHR of chitosan at 15,780 and 16,380 cm^{-1}, respectively. Furthermore, the FTIR peak ranging from 3,500 to 3,300 cm^{-1} was attributed to the O-H group of chitosan. The FTIR spectrum for RA indicated the presence of absorption bands of the carbonyl group at 1,685 cm^{-1} and aliphatic alkanes at approximately 2,900 cm^{-1}. In the RACHNP spectra, an additional absorption band appearing at 1,704 cm^{-1} demonstrates the conjugation between RA and CHNPs. Lastly, the presence of other reference bands of RA and CHNPs indicates the formation of an RACHNP copolymer, resulting from the interaction between the RA carbonyl group and the chitosan amino group.

3. Loading capacity of CHNPs

First, the standard curve of ultraviolet absorbance was calculated for RA. Then, the equation relating the optical density (OD) and the concentration (C) of RA was determined, as displayed below:

$$OD = 0.0106C + 0.0403 \ (R^2 = 0.9888)$$

Based on the equation, the LC% of RA for RACHNPs was 50.97% (Figure 1B).

Table 2. Size and zeta potential of CHNP and RACHNP

Sample	Size ± SD (nm)	Zeta potential (mV)
CHNP	228 ± 22.78	32.6
RACHNP	324 ± 29.9	10.8

CHNP, chitosan nanoparticle; RACHNP, retinoic acid loaded with chitosan nanoparticle; SD, standard deviation.

Table 1. Primers used

Genes	Primer sequences	Product length (nt)	TM (°C)
Bax	F: GGATGATTGCTGACGTGGAC	91	58
	R: CCCCAGTTGAAGTTGCCATC		
Bcl2	F: TCGCAGAGATGTCCAGTCAG	92	58
	R: CACCCCATCCCTGAAGAGTT		
P53	F: ACCCTGGCACCTACAATGAA	102	58
	R: TGGAAGGAAAGTAGGCCCTG		
Fas	F: ACCTCAGTTCCAGCCATGAA	111	60
	R: TGCTGGCAAAGAGAACACAC		
FasL	F: GAACCGCTCTGATCTCTGGA	117	60
	R: GCTGGTTGTTGCAAGACTGA		

nt, nucleotide; TM, melting temperature; F, forward; R, reverse.

F Mazini et al.   Retinoic acid loaded chitosan nanoparticles improve spermatogenesis

CERM

4. *In vitro* release of RA from CHNPs

Figure 1C illustrates the cumulative release of RA from RACHNPs over a span of 120 hours. The RA release rate was 59.3% within this period, with approximately half of this release taking place in the initial 60 hours. This is attributed to the quantity of RA absorbed on the CHNP surface. The release rate then proceeded more slowly over the subsequent hours, which is associated with the amount of RA embedded in the CHNP matrix.

5. Effects of RA, CHNPs, and RACHNPs on sperm parameters

The total number of spermatozoa was significantly lower in the Hyp group than in the RA, CHNP, and RACHNP groups ($p < 0.001$ for all). The total numbers of spermatozoa in the RA, CHNP, and Hyp groups were significantly lower than in the control group ($p < 0.001$), but the sperm count in the RACHNP group did not significantly differ from that in the control group. A significant difference was observed between the RACHNP and both the CHNP and RA groups. The data also showed a higher rate of improvement in the group treated with RACHNPs compared to the RA and CHNP groups (Figure 2A). Relative to the control group, sperm viability was significantly lower in the Hyp group ($p < 0.001$), but no significant difference was observed between the Hyp and CHNP groups. The proportion of viable sperm in the RA and RACHNP groups was statistically higher than in the Hyp group ($p < 0.001$ for both). Sperm viability in the RA group was significantly lower than in the control group ($p < 0.001$), but no significant difference was found between the RACHNP and control groups (Figure 2B). The study results showed a statistically significant decrease in sperm motility in the Hyp group compared to the control group ($p < 0.001$). Statistically significant differences were also observed in sperm motility between the CHNP, RA, and RACHNP groups and the Hyp group ($p < 0.01$, $p < 0.001$, and $p < 0.001$, respectively). The groups treated with CHNPs, RA, and RACHNPs showed greater increases in sperm motility relative to the Hyp group, but no significant difference was noted between the RACHNP and control groups (Figure 2C). Sperm morphology in the Hyp group was significantly poorer than in the RA, RACHNP, and control groups ($p < 0.001$). A significant difference in sperm morphology was observed between the RACHNP and CHNP groups, but no significant difference was found between the RACHNP, RA, and control groups (Figure 2D).
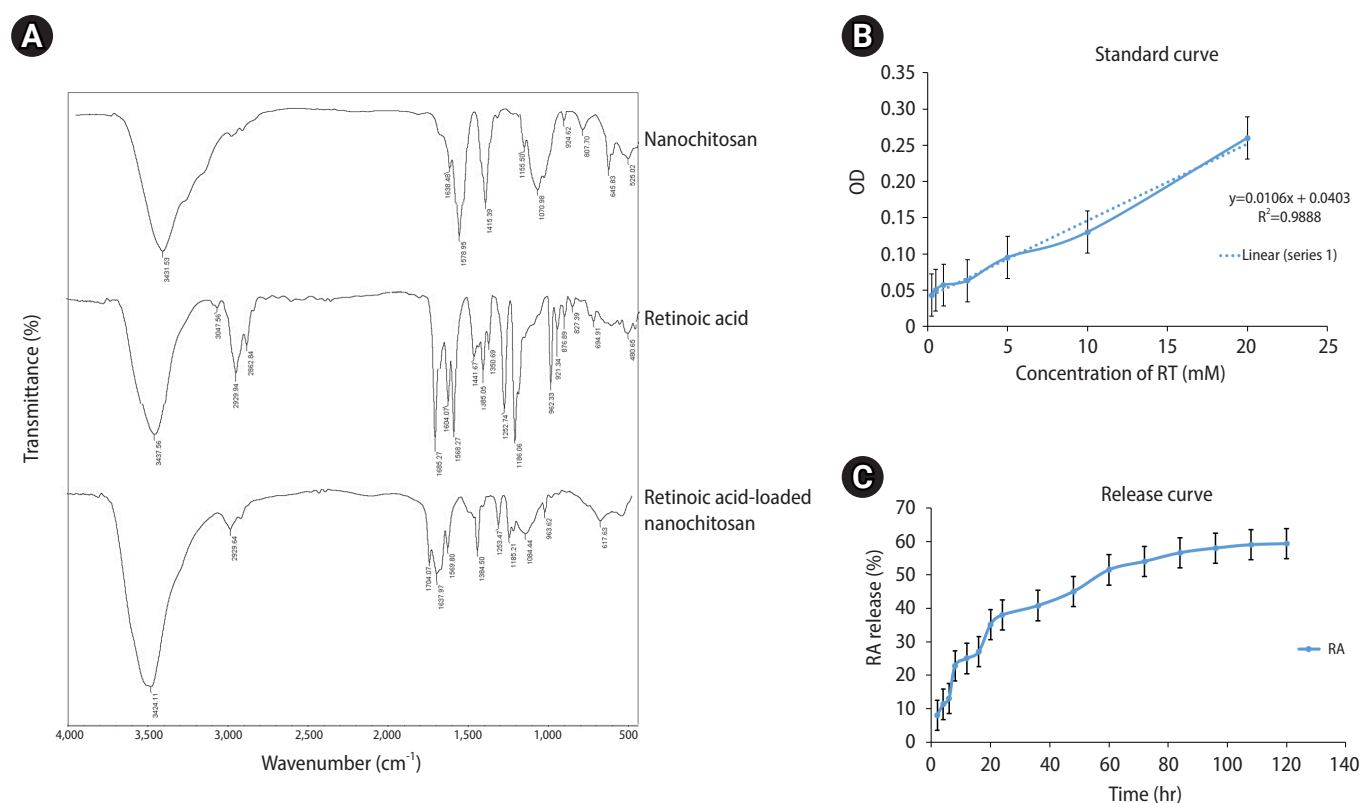

Figure 1. (A) Fourier-transform infrared spectroscopy analysis of chitosan nanoparticles, retinoic acid, and retinoic acid loaded chitosan nanoparticles. (B) Standard curve of retinoic acid ultraviolet absorbance. (C) *In vitro* release profile of retinoic acid from chitosan nanoparticles. OD, optical density; RA, retinoic acid.
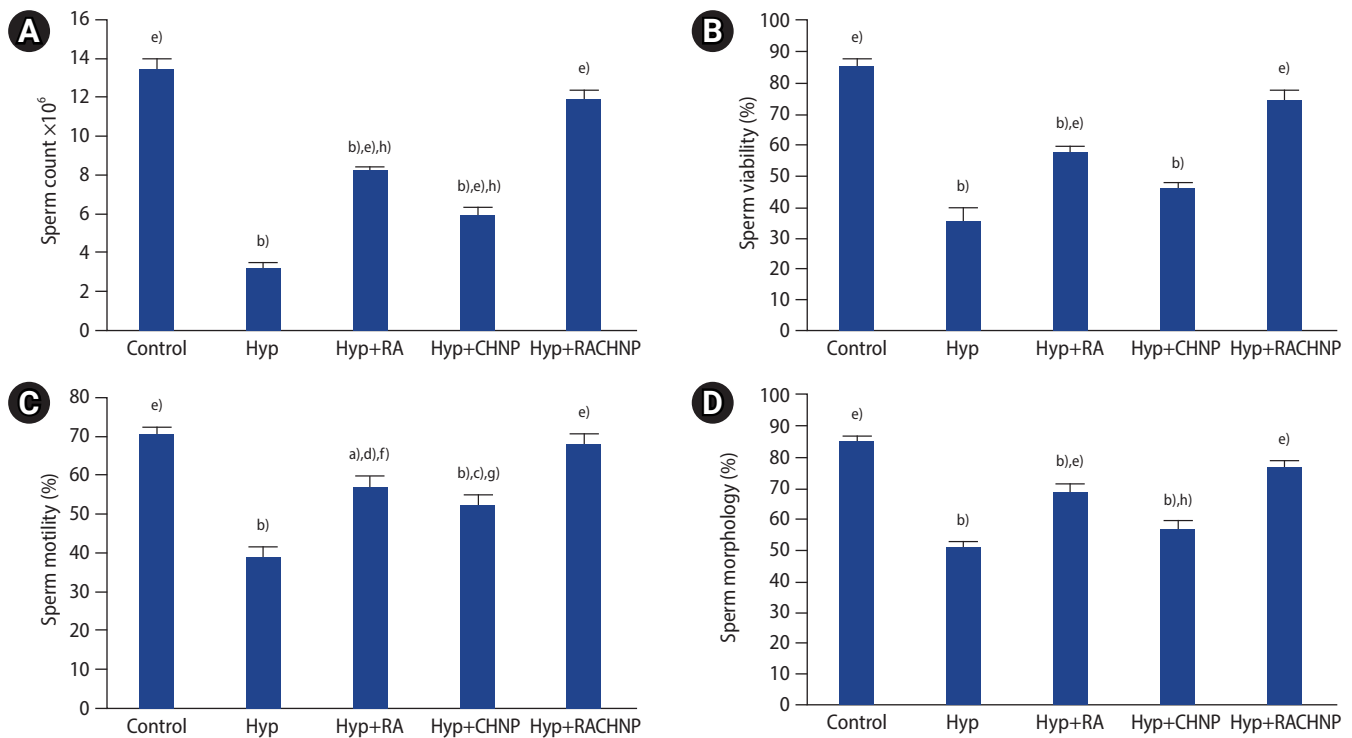
Figure 2. Effects of retinoic acid (RA), chitosan nanoparticle (CHNP), and retinoic acid loaded with chitosan nanoparticle (RACHNP) administration on sperm parameters. (A) Sperm count. (B) Sperm morphology. (C) Sperm motility. (D) Sperm viability. Data are presented as mean±standard error. Hyp, scrotal hyperthermia. [a]$p<0.01$ and [b]$p<0.001$ compared to the control group; [c]$p<0.05$, [d]$p<0.01$, and [e]$p<0.001$ compared to the Hyp group; [f]$p<0.05$, [g]$p<0.01$, and [h]$p<0.001$ compared to the RACHNP group.

6. Effects of RA, CHNPs, and RACHNPs on serum testosterone levels

The hormone assay revealed a decrease in serum testosterone concentration in animals subjected to Hyp, compared to both the control and RACHNP groups ($p<0.001$, $p<0.05$). Our findings indicated no significant difference in serum testosterone levels between the RA and CHNP groups and the Hyp group. However, a significant difference was observed between the RACHNP group and the control group ($p<0.05$). Additionally, significant differences were found when comparing the RACHNP group to both the CHNP and RA groups ($p<0.01$ and $p<0.05$, respectively) (Figure 3A).

7. Effects of RA, CHNPs, and RACHNPs on ROS measurement

The data revealed significant increases in ROS levels in the Hyp group when compared to the RACHNPs, RA, and control groups ($p<0.001$, $p<0.001$, $p<0.001$) based on testis tissue measurements. Furthermore, the results indicated that ROS levels were notably lower in the RACHNP and RA groups than in the Hyp group ($p<0.001$). However, no significant difference was present between the Hyp and CHNP groups. The ROS measurements revealed a statistically significant difference between the RA and control groups ($p<0.05$), but no such difference was found between the RACHNP and control groups.

Additionally, our results showed a significant difference between the RACHNP therapy group and the CHNP group, but no significant difference was observed between the RACHNP and RA groups (Figure 3B).

8. Effects of RA, CHNPs, and RACHNPs on stereological parameters

Stereological test results revealed a significantly reduced testicular volume in the Hyp group compared to the control group ($p<0.001$). While the RACHNP treatment group showed a statistically significant increase in testicular volume compared to the Hyp group ($p<0.001$), no difference was observed between the Hyp group and the RA or CHNP treatment groups. Similarly, no significant change in testicular volume was detected between the RACHNP and control groups (Figures 4 and 5A).

The findings revealed a significantly lower count of spermatogonia in the Hyp group compared to both the control and RACHNP groups ($p<0.001$ for both). No statistically significant difference was found in the number of spermatogonia between either the RA or CHNP groups and the Hyp group. Although RACHNP treatment significantly increased the count of spermatogonia, it did not reach the level observed in the control group (Figure 5B).

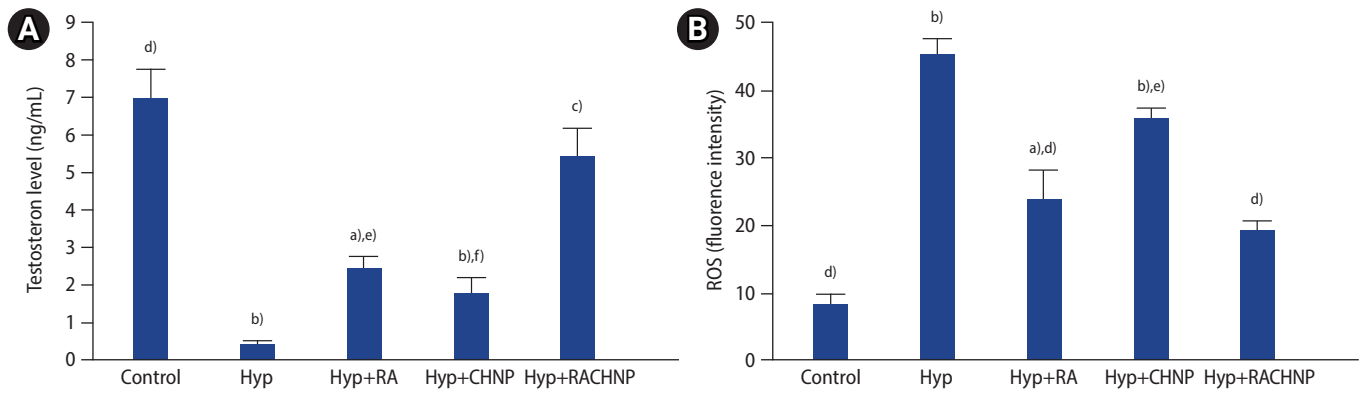Stereological data revealed a significant decrease in the number of

F Mazini et al.   Retinoic acid loaded chitosan nanoparticles improve spermatogenesis

CERM

Figure 3. Effects of retinoic acid (RA), chitosan nanoparticle (CHNP), and retinoic acid loaded with chitosan nanoparticle (RACHNP) administration on: (A) testosterone hormone levels across groups. (B) Reactive oxygen species (ROS) level across groups (n=6). Data are presented as mean±standard error. Hyp, scrotal hyperthermia. [a]$p<0.01$ and [b]$p<0.001$ compared to the control group; [c]$p<0.01$ and [d]$p<0.001$ compared to the Hyp group; [e]$p<0.05$ and [f]$p<0.01$ compared to the RACHNP group.
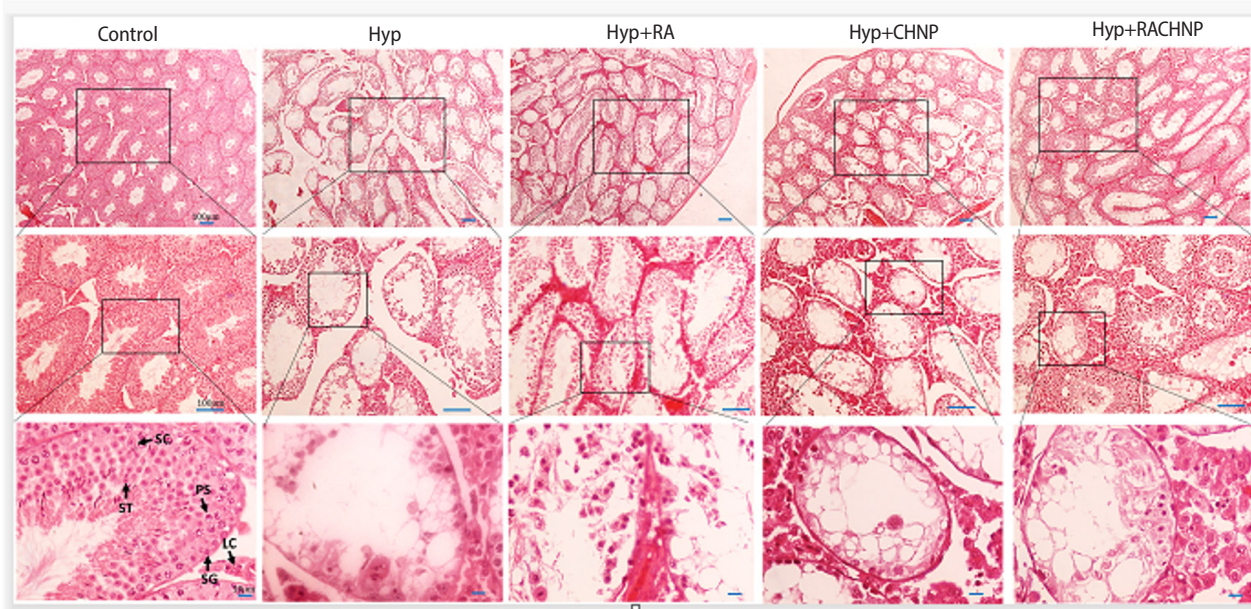

Figure 4. Photomicrograph of the testis stained with hematoxylin and eosin (×4, ×10, and ×40) in the study groups. Histological findings showed normal spermatogenesis in the control group. Testicular tissue showed impaired spermatogenesis with degeneration of seminiferous tubules in the scrotal hyperthermia (Hyp) group and improvement in the retinoic acid loaded with chitosan nanoparticle (RACHNP) group. RA, retinoic acid; CHNP, chitosan nanoparticle; SC, Sertoli cell; ST, spermatid; PS, primary spermatocyte; LC, Leydig cell; SG, spermatogonia.

primary spermatocytes in the Hyp group compared to the control and RACHNP groups ($p<0.001$). However, the number of primary spermatocytes in the Hyp group did not significantly differ from those in the RA and CHNP groups. Interestingly, the RACHNP group exhibited a notable increase in the number of primary spermatocytes relative to the RA and CHNP groups ($p<0.001$ for both). These results suggest that RACHNPs significantly mitigated the detrimental effects of heat stress (Figure 5C). The data also indicated a significant

decrease in the number of round spermatids in the testis tissue of the Hyp group compared to the control and RACHNP groups ($p<0.001$ for both). While the RACHNP group showed a notable increase in the number of round spermatids, this increase was not statistically significant relative to the control group (Figure 5D).

The findings indicate a significant decrease in the number of Leydig cells in the Hyp group when compared to both the RACHNP ($p<0.001$) and control ($p<0.001$) groups. Conversely, the RACHNP
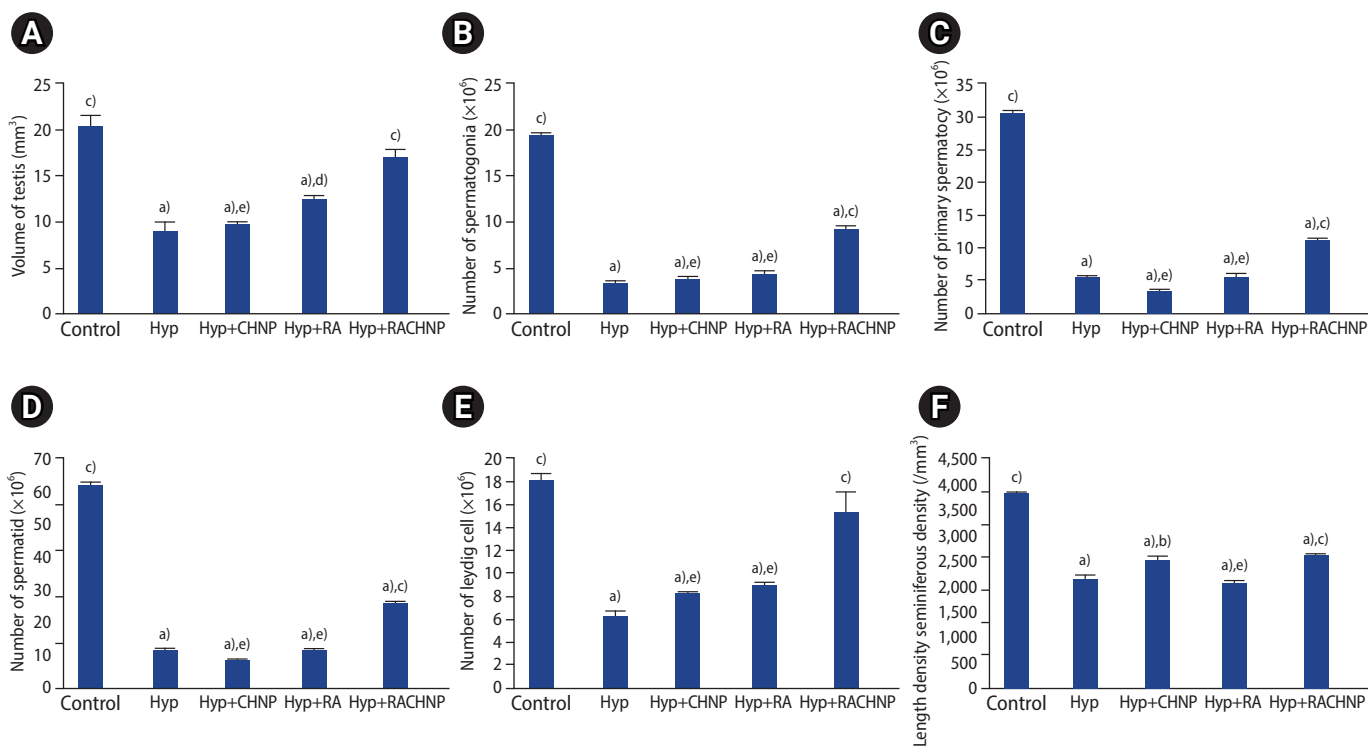
Figure 5. Effects of retinoic acid (RA), chitosan nanoparticle (CHNP), and retinoic acid loaded with chitosan nanoparticle (RACHNP) administration on stereological parameters: (A) testis volume, (B) number of spermatogonia, (C) number of primary spermatocytes, (D) number of spermatids, (E) number of Leydig cells, and (F) seminiferous tubule length in scrotal hyperthermia (Hyp)-induced mice (n=6). Data are presented as mean±standard error. [a)]$p < 0.0001$ compared to the control group; [b)]$p < 0.01$ and [c)]$p < 0.001$ compared to the Hyp group; [d)]$p < 0.01$ and [e)]$p < 0.001$ compared to the RACHNP group.

treatment group demonstrated an increase in the number of Leydig cells, with no significant difference observed between the RACHNP and control groups (Figure 5E).

The length of the seminiferous tubules was significantly shorter in the Hyp group compared to the control, RACHNP, and RA groups ($p < 0.001$, $p < 0.001$, and $p < 0.01$, respectively). Relative to the Hyp group, an increase was observed in the length of the seminiferous tubules after the mice were administered RA and RACHNPs (Figure 5F). The statistical data indicated that the total count of Sertoli cells remained consistent across all study groups. The Sertoli cells demonstrated resilience to the rising temperature within the testis.

9. Effects of RA, CHNPs, and RACHNPs on immunohistochemical staining

The percentage of apoptotic factor immunoreactivity in testicular cells was assessed using immunohistochemical (IHC) staining. Figure 6 illustrates the caspase-3 immunoreactivity in testicular tissues after the induction of Hyp. A significant increase in caspase-3 immunoreactivity was observed in the Hyp group compared to the control ($p < 0.001$), RA ($p < 0.01$), RACHNP ($p < 0.001$), and CHNP ($p < 0.01$) groups. Additionally, a significant increase in apoptosis was noted in

the RA and CHNP groups compared to the control group ($p < 0.01$ for both). However, no significant difference was found between the RACHNP and control groups. In this study, a significant difference was noted between the RACHNP group and both RA and CHNP groups ($p < 0.05$ for both) (Figure 6).

10. Effects of RA, CHNPs, and RACHNPs on qRT-PCR findings

The relative messenger RNA (mRNA) expression levels of *Bax*, *bcl2*, *p53*, *Fas*, and *FasL* were normalized to the control and quantified across different groups. As indicated in Table 3, the Hyp group exhibited a significant increase in the relative mRNA expression levels of *p53*, *Fas*, and *FasL* compared to the control group ($p < 0.001$, $p < 0.05$, and $p < 0.01$, respectively) (Table 3). The statistical analysis revealed that the expression level of *Bax* was elevated in the Hyp group compared to both the RA and RACHNP groups ($p < 0.05$ for both). The expression of *p53* was also higher in the Hyp group compared to the control, RA, CHNP, and RACHNP groups ($p < 0.001$ for all). Similarly, *Fas* expression was increased in the Hyp group compared to the control, CHNP, RA, and RACHNP groups ($p < 0.05$, $p < 0.05$, $p < 0.01$, and $p < 0.01$, respectively). *FasL* expression was also elevated in the Hyp group compared to the control, CHNP, RA,
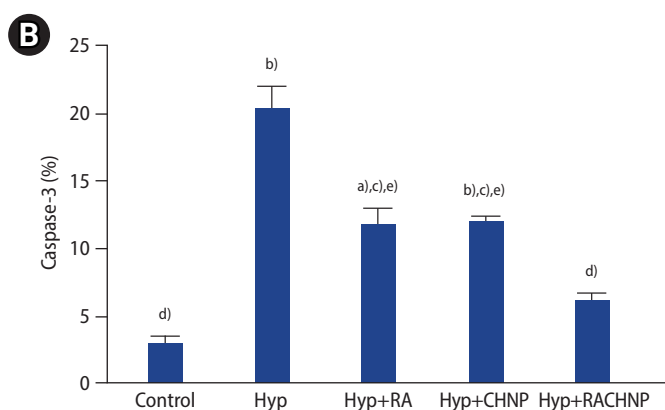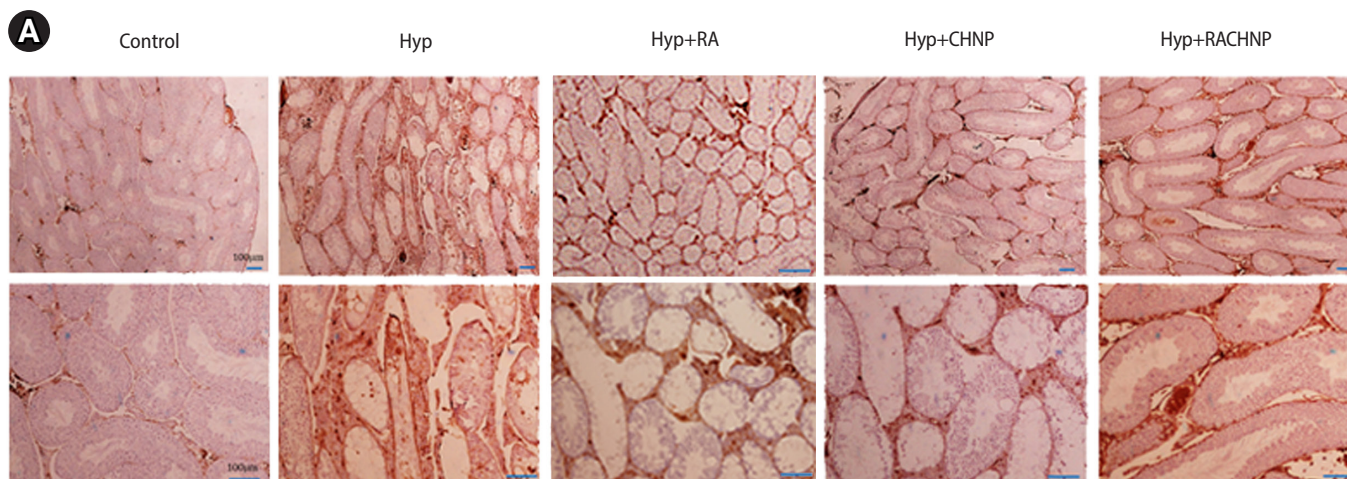
F Mazini et al. Retinoic acid loaded chitosan nanoparticles improve spermatogenesis

CERM

Figure 6. (A) Photomicrograph of immunohistochemistry (IHC) staining of the testis for caspase-3 in the study groups (n=6). (B) Effects of retinoic acid (RA), chitosan nanoparticle (CHNP), and retinoic acid loaded with chitosan nanoparticle (RACHNP) administration on IHC results. Data are presented as mean±standard error. Hyp, scrotal hyperthermia. [a]$p<0.01$ and [b]$p<0.001$ compared to the control group; [c]$p<0.01$ and [d]$p<0.001$ compared to the Hyp group; [e]$p<0.05$ compared to the RACHNP group.

Table 3. mRNA expression levels of *Bax, p53, Fas, FasL,* and *Bcl2* in the testis across groups

Group	P53	Bax	Fas	FasL	Bcl2
Control	1±0.00[f]	1±0.00	1±0.00[d]	1±0.00[e]	1±.00[f]
Hyp	7.53±0.305[c]	3.44±0.80	4.15±0.54[a]	4.47±0.54[b),f]	0.005±0.00015[c]
CHNP	0.18±0.12[f]	1.25±0.76	1.03±0.71[d]	0.34±0.17[f]	0.015±0.003[c]
RA	0.015±0.001[a),f]	0.25±0.05[d]	0.17±0.009[e]	0.098±0.022[f]	0.105±0.050[c]
RACHNP	0.012±0.005[a),f]	0.012±0.007[d]	0.05±0.04[e]	0.040±0.0048[f]	0.118±0.023[c]

Values are presented as mean±standard error.

mRNA, messenger RNA; Hyp, scrotal hyperthermia; CHNP, chitosan nanoparticle; RA, retinoic acid; RACHNP, retinoic acid loaded with chitosan nanoparticle.
[a]$p<0.05$, [b]$p<0.01$, and [c]$p<0.001$ in comparison to the control group; [d]$p<0.05$, [e]$p<0.01$, and [f]$p<0.001$ compared to the Hyp group.

and RACHNP groups ($p<0.01$, $p<0.01$, $p<0.001$, and $p<0.001$, respectively). In contrast, the mRNA expression level of *bcl2* was reduced in the Hyp group compared to the control group ($p<0.001$). A significant difference was found in the expression level of *bcl2* between the control group and all other groups ($p<0.001$) (Table 3).

Discussion

In line with previous studies on the effects of heat stress on spermatogenesis [11,34], our research found that Hyp leads to reproductive toxicity and azoospermia in animals. The sperm parameter analysis showed significant improvements in sperm count, motility, viability, morphology, and serum testosterone levels, along with a noticeable decrease in ROS production levels in animals treated with RACHNPs. Additionally, substantial improvements were observed in testis volume, seminiferous tubule length, and testicular cell count in the group that received RACHNPs. A reduction in the caspase-3 protein expression level was also noted in animals treated with RACHNPs. This study presents the first evidence of the increased effectiveness of RACHNPs in alleviating testicular damage caused by

hyperthermia in mice.

CHNP formulations appear to be an ideal slow release mechanism for drugs with unfavorable kinetics, such as RA. Formulations with a high RA load often display a delayed drug release profile. Techniques for delivering RA help to overcome challenges such as poor solubility in water, a short half-life of only a few hours, and adverse side effects like dryness, headaches, and hypertriglyceridemia when administered in high doses [35,36]. Studies have shown that considerable plasma levels of RACHNPs persist for a longer duration following IP delivery compared to administration without RA. RA is a free radical scavenger with antioxidant properties. Both laboratory and animal studies have demonstrated that RACHNPs are more effective than RA-free formulations in enhancing the antioxidant effects of RA [37].

The histological analysis revealed that Hyp led to a decrease in the count of spermatogonia, primary spermatocytes, and round spermatids. It also caused atrophic changes in the seminiferous tubules, including the degeneration, reduction, and disorganization of germ cells. Additionally, Leydig cells in the interstitial tissues underwent degeneration, developed small to large vacuoles, and displayed irregular gaps; additionally, a significant decrease in testicular volume was observed [3,11,38]. However, the injection of RACHNPs restored the spermatogenic processes, testis weight, testicular histoarchitecture, and pathophysiological parameters in the testes affected by Hyp. Neither CHNPs nor the absence of RA yielded positive results in the testicular cells of the heat-stressed group, suggesting that RACHNPs could rectify the spermatogenesis abnormalities induced by Hyp. The present study showed that RACHNPs significantly enhanced the proliferation of germ cells, resulting in increases in the number of spermatogonia, primary spermatocytes, and round spermatids. Consistent with previous studies, long-term Hyp inflicted severe damage on the testis tissue. The antioxidative properties of RACHNPs and their protective effects on mitochondria may be the key factors in counteracting the effects of heat stress and restoring spermatogenesis following RACHNP consumption.

Heat stress, or hyperthermia, can negatively impact the function of Leydig cells and the production of testosterone. This aligns with previous research that has shown a dramatic decrease in serum testosterone levels due to heat stress [39,40]. However, treatment with RACHNPs can counteract the reproductive damage caused by heat exposure in male mice. This treatment regulates Leydig cell steroidogenesis, leading to an increase in testosterone levels. The observed increase in testosterone levels in mice treated with RACHNPs underscores its potential to mitigate the reproductive toxicity caused by heat stress. Consequently, RACHNPs enhance spermatogenesis and reduce testicular dysfunction arising from heat exposure.

IHC analysis was performed to detect caspase-3 and illustrate apoptosis in the seminiferous tubules. Hyp heightened the immunoreactivity of sperm cells to caspase-3, suggesting that oxidative stress induced by hyperthermia could result in cell death. However, the application of RA, CHNPs, and RACHNPs mitigated the apoptotic damage instigated by hyperthermia. Prior research has indicated that CHNP may aid in alleviating testicular damage by diminishing antiapoptotic activity [41]. Meanwhile, RA, functioning as an antioxidant, can neutralize free radicals and impede apoptosis to safeguard spermatogenic cells [42,43]. In the current study, mice treated with RACHNPs did not exhibit significant differences from the control group, while mice treated with RA and CHNPs demonstrated notable differences compared to the control group.

Interestingly, treatment with RACHNPs led to a decrease in the localization of the caspase-3 immunoreactive protein, which suggests a reduction in apoptotic cells. This observation implies that RACHNPs have a strong antioxidant activity and are more effective at scavenging free radicals than RA alone. Furthermore, RACHNPs may employ a unique method of cellular internalization, triggering a more potent antiapoptotic response than that elicited by RA alone. The diminished efficacy of RA, when compared to RACHNPs, could be attributed to its short half-life and swift conversion to an inactive metabolite. In contrast, RACHNPs exhibit a longer lifespan and increased effectiveness.

Previous research has demonstrated that elevated temperatures significantly increase the production of caspase-3 mRNA and the amount of cleaved caspase-3 protein [44]. However, the application of RA therapy has been found to significantly reduce the increase in cleaved caspase-3 protein levels and caspase-3 mRNA expression caused by heat stress [45]. These results imply that RACHNPs could potentially inhibit the caspase-3–mediated apoptosis pathway, thereby reducing cell death. This conclusion aligns with our own research findings [46]. Caspase-3, a common executor of cell death, is crucial for the induction of apoptosis by heat stress.

Research has established a strong link between oxidative stress caused by ROS and both death receptor-mediated and mitochondrial-mediated apoptosis. Numerous studies suggest that ROS contributes to heat-induced apoptosis by encouraging ROS accumulation. Our research suggests that heat significantly increases the buildup of ROS in testicular cells. However, treatment with RA and RACHNPs notably decreases the increase in ROS$^+$ cell count and ROS concentration triggered by thermal stress. We observed that mice treated with RACHNPs showed no significant differences from the control group, while the RA and CHNP groups displayed considerable differences compared to the control group. This could be due to the antioxidant properties of RA and CHNPs.

Rao et al. [47] found that RA enhanced the activity of superoxide dismutase (SOD) and decreased the production of malondialdehyde (MDA) in rats, thereby mitigating the effects of hepatic ischemia/reperfusion injury. Similarly, Khafaga and El-Sayed [45] discovered

F Mazini et al.   Retinoic acid loaded chitosan nanoparticles improve spermatogenesis

CERM

that all-*trans*-retinoic acid (ATRA) lessened the amount of MDA and alleviated doxorubicin-induced cardiac oxidative damage in rats by promoting the activities of antioxidant enzymes such as glutathione peroxidase, SOD, and catalase (CAT). A previous study revealed that RA treatment significantly elevated the activities of SOD, CAT, and total antioxidant capacity, while also reducing MDA levels. That study also examined the cellular expression of genes associated with antioxidants, finding that RA diminished oxidative stress related to cell damage by improving antioxidant capacity [48]. RACHNPs, known for their antioxidant properties, have the potential to actively inhibit apoptosis in spermatogenic cells and perform free radical scavenging functions.

Furthermore, several apoptotic signaling pathways, including the mitogen-activated protein kinase (MAPK) and p53 pathways, have been associated with ROS. To determine whether the P38MAPK signaling pathway plays a role in the mechanism by which ATRA reduces cell apoptosis, researchers used Western blot analysis to assess the level of P38MAPK phosphorylation. Prior research has shown that damaged cells display a significant increase in P38MAPK phosphorylation. The findings of this study suggest that ATRA effectively mitigates cellular damage caused by oxidative stress and ROS by inhibiting the P38MAPK signaling pathway. However, further research is needed to definitively confirm whether ATRA inhibits the ROS-mediated P38MAPK signaling pathway, thereby reducing cellular damage and apoptosis [47]. Antioxidant supplements, such as RA and RACHNPs, could potentially shield against the detrimental effects of high ROS production caused by testicular hyperthermia. The primary ROS species, including superoxide anion, hydroxyl radical, and hydrogen peroxide, may be absorbed by RACHNPs via their amino group chelation sites. The positive charges present in the RACHNP complex may allow it to neutralize negatively charged radicals, such as superoxide and hydroxyl.

We examined the relative mRNA expression levels of the *bax*, *p53*, *Fas*, and *FasL* genes in testicular tissue due to the extensive cell death observed at 43 °C. Our findings revealed that mice subjected to high temperatures exhibited increased transcription levels of these genes compared to the control group. Furthermore, we found that animals subjected to Hyp demonstrated reduced relative levels of *bcl2* mRNA expression. Following heat treatment, we observed evidence of the upregulation of the *p53*, *Fas*, and *FasL* proteins, along with the downregulation of *bcl2*.

We observed that mice treated with RA and RACHNPs exhibited reduced apoptosis when exposed to heat. Our findings indicated that the expression levels of apoptotic genes in the RA and RACHNP treatment groups were lower than those in the control group. This could be attributed to the increased expression of the *hsp90* and *hsp70* genes during hyperthermia. These genes possess antiapop-

totic properties, which are further enhanced by the antiapoptotic effects of RA and RACHNP [49,50].

In conclusion, the results of this study indicate that the RACHNP formulation is biocompatible and shows superior effectiveness in reducing Hyp in male mice, compared to free RA. The protective impact of this formulation on spermatogenesis underscores the potential of CHNPs as an effective nanocarrier for RA delivery. The increased therapeutic effectiveness of RACHNPs could be due to their enhanced absorption and sustained-release properties, as previously discussed. Therefore, the RACHNP formulation could serve as a promising alternative to traditional RA formulations and CHNP-based treatments for male infertility. These findings are likely to stimulate further research into the protective role of RACHNPs in male reproductive health.

Conflict of interest

Acknowledgments

ORCID

Fatemeh Mazini	https://orcid.org/0000-0001-8843-4310
Mohammad-Amin Abdollahifar	
	https://orcid.org/0000-0001-6947-3285
Hassan Niknejad	https://orcid.org/0000-0001-7736-1232
Asma Manzari-Tavakoli	https://orcid.org/0000-0003-1146-644X
Mohsen Zhaleh	https://orcid.org/0000-0003-0623-1689
Reza Asadi-Golshan	https://orcid.org/0000-0003-1901-7171
Ali Ghanbari	https://orcid.org/0000-0002-8080-2809

Author contributions

Conceptualization: FM. Data curation: HN. Formal analysis: AMT. Funding acquisition: MZ, Methodology: RAG. Project administration: AG, Writing-original draft: MAA. Writing-review & editing: RAG.

References

1. Abdelhamid MH, Walschaerts M, Ahmad G, Mieusset R, Bujan L,

Hamdi S. Mild experimental increase in testis and epididymis temperature in men: effects on sperm morphology according to spermatogenesis stages. Transl Androl Urol 2019;8:651-65.

2. Wu YQ, Rao M, Hu SF, Ke DD, Zhu CH, Xia W. Effect of transient scrotal hyperthermia on human sperm: an iTRAQ-based proteomic analysis. Reprod Biol Endocrinol 2020;18:83.

3. Afshar A, Aliaghaei A, Nazarian H, Abbaszadeh HA, Naserzadeh P, Fathabadi FF, et al. Curcumin-loaded iron particle improvement of spermatogenesis in azoospermic mouse induced by long-term scrotal hyperthermia. Reprod Sci 2021;28:371-80.

4. Jeremy M, Kharwar RK, Roy VK. Synthetic leptin c-fragment peptide minimizes heat-induced impairment of spermatogenesis in mice via Stat3 signalling. Theriogenology 2022;178:40-9.

5. Dong G, Zhou H, Gao Y, Zhao X, Liu Q, Li Z, et al. Effects of 1.5-GHz high-power microwave exposure on the reproductive systems of male mice. Electromagn Biol Med 2021;40:311-20.

6. Parivar K, Shakiba S, Hekmat A. Effect of fourth generation of mobile phone standards (4G) on spermatogenesis and testis tissue of NMRI rats. Res Cell Tissue 2021;1:25-32.

7. Jensen CFS, Ostergren P, Dupree JM, Ohl DA, Sonksen J, Fode M. Varicocele and male infertility. Nat Rev Urol 2017;14:523-33.

8. Kang C, Punjani N, Lee RK, Li PS, Goldstein M. Effect of varicoceles on spermatogenesis. Semin Cell Dev Biol 2022;121:114-24.

9. Abdelhamid MH, Esquerre-Lamare C, Walschaerts M, Ahmad G, Mieusset R, Hamdi S, et al. Experimental mild increase in testicular temperature has drastic, but reversible, effect on sperm aneuploidy in men: a pilot study. Reprod Biol 2019;19:189-94.

10. Gao Y, Wang C, Wang K, He C, Hu K, Liang M. The effects and molecular mechanism of heat stress on spermatogenesis and the mitigation measures. Syst Biol Reprod Med 2022;68:331-47.

11. Ziaeipour S, Piryaei A, Aliaghaei A, Nazarian H, Naserzadeh P, Ebrahimi V, et al. Chronic scrotal hyperthermia induces azoospermia and severe damage to testicular tissue in mice. Acta Histochem 2021;123:151712.

12. Mardani M, Vaez A, Razavi S. Effect of saffron on rat sperm chromatin integrity. Iran J Reprod Med 2014;12:343-50.

13. Karimi A, Behmard V, Toghiani S, Moravej FS. The study of the protective effect of vitamin E and retinoic acid on testicular tissue in mice treated with cyclophosphamide. Arch Med Lab Sci 2020; 6:e9.

14. Da Silva F, Jian Motamedi F, Weerasinghe Arachchige LC, Tison A, Bradford ST, Lefebvre J, et al. Retinoic acid signaling is directly activated in cardiomyocytes and protects mouse hearts from apoptosis after myocardial infarction. Elife 2021;10:e68280.

15. Khanehzad M, Abbaszadeh R, Holakuyee M, Modarressi MH, Nourashrafeddin SM. FSH regulates RA signaling to commit spermatogonia into differentiation pathway and meiosis. Reprod Biol

Endocrinol 2021;19:4.

16. Ghyselinck NB, Duester G. Retinoic acid signaling pathways. Development 2019;146:dev167502.

17. Schleif MC, Havel SL, Griswold MD. Function of retinoic acid in development of male and female gametes. Nutrients 2022;14:1293.

18. Zhou Y, Wang Y. Action and interaction between retinoic acid signaling and blood-testis barrier function in the spermatogenesis cycle. Cells 2022;11:352.

19. Li H, Palczewski K, Baehr W, Clagett-Dame M. Vitamin A deficiency results in meiotic failure and accumulation of undifferentiated spermatogonia in prepubertal mouse testis. Biol Reprod 2011; 84:336-41.

20. Jeong YI, Kim DG, Jang MK, Nah JW, Kim YB. All-trans retinoic acid release from surfactant-free nanoparticles of poly (DL-lactide-co-glycolide). Macromol Res 2008;16:717-24.

21. Farzamfar S, Hasanpour A, Nazeri N, Razavi H, Salehi M, Shafei S, et al. Extracellular micro/nanovesicles rescue kidney from ischemia-reperfusion injury. J Cell Physiol 2019;234:12290-300.

22. Jangjou A, Meisami AH, Jamali K, Niakan MH, Abbasi M, Shafiee M, et al. The promising shadow of microbubble over medical sciences: from fighting wide scope of prevalence disease to cancer eradication. J Biomed Sci 2021;28:49.

23. Falchi L, Khalil WA, Hassan M, Marei WF. Perspectives of nanotechnology in male fertility and sperm function. Int J Vet Sci Med 2018;6:265-9.

24. Naseri-Nosar M, Farzamfar S, Salehi M, Vaez A, Tajerian R, Azami M. Erythropoietin/aloe vera-releasing wet-electrospun polyvinyl alcohol/chitosan sponge-like wound dressing: in vitro and in vivo studies. J Bioact Compat Polym 2018;33:269-81.

25. Abbaszadeh-Goudarzi G, Haghi-Daredeh S, Ehterami A, Rahmati M, Nazarnezhad S, Hashemi SF, et al. Evaluating effect of alginate/chitosan hydrogel containing 4-Methylcatechol on peripheral nerve regeneration in rat model. Int J Polym Mater Polym Biomater 2021;70:1248-57.

26. Azizian S, Hadjizadeh A, Niknejad H. Chitosan-gelatin porous scaffold incorporated with chitosan nanoparticles for growth factor delivery in tissue engineering. Carbohydr Polym 2018;202:315-22.

27. Gheisari F, Shafiee M, Abbasi M, Jangjou A, Izadpanah P, Vaez A, et al. Janus nanoparticles: an efficient intelligent modern nanostructure for eradicating cancer. Drug Metab Rev 2021;53:592-603.

28. Manzari-Tavakoli A, Tarasi R, Sedghi R, Moghimi A, Niknejad H. Fabrication of nanochitosan incorporated polypyrrole/alginate conducting scaffold for neural tissue engineering. Sci Rep 2020; 10:22012.

29. Wang F, He S, Chen B. Retinoic acid-loaded alginate microspheres as a slow release drug delivery carrier for intravitreal treatment. Biomed Pharmacother 2018;97:722-8.

F Mazini et al.   Retinoic acid loaded chitosan nanoparticles improve spermatogenesis

CERM

30. Yucel C, Arslan FD, Ekmekci S, Ulker V, Kisa E, Erdogan Yucel E, et al. Protective effect of all-trans retinoic acid in cisplatin-induced testicular damage in rats. World J Mens Health 2019;37:249-56.

31. Ziaeipour S, Rezaei F, Piryaei A, Abdi S, Moradi A, Ghasemi A, et al. Hyperthermia versus busulfan: finding the effective method in animal model of azoospermia induction. Andrologia 2019;51: e13438.

32. Panahi S, Karamian A, Sajadi E, Aliaghaei A, Nazarian H, Abdi S, et al. Sertoli cell-conditioned medium restores spermatogenesis in azoospermic mouse testis. Cell Tissue Res 2020;379:577-87.

33. Ziaeipour S, Ahrabi B, Naserzadeh P, Aliaghaei A, Sajadi E, Abbaszadeh HA, et al. Effects of sertoli cell transplantation on spermatogenesis in azoospermic mice. Cell Physiol Biochem 2019;52: 421-34.

34. Khosravi A, Hasani A, Behnam P, Piryaei A, Pirani M, Aliaghaei A, et al. An effective method for establishing animal models of azoospermia and oligospermia. Andrologia 2021;53:e14095.

35. Errico C, Gazzarri M, Chiellini F. A novel method for the preparation of retinoic acid-loaded nanoparticles. Int J Mol Sci 2009;10:2336-47.

36. Ferreira R, Napoli J, Enver T, Bernardino L, Ferreira L. Advances and challenges in retinoid delivery systems in regenerative and therapeutic medicine. Nat Commun 2020;11:4265.

37. Chae JM, Oh IJ. Sustained release of all-trans retinoic acid from chitosan-coated poly (DL-lactide-co-glycolide) nanoparticles. Yakhak Hoeji 2019;63:367-73.

38. Ilkhani S, Moradi A, Aliaghaei A, Norouzian M, Abdi S, Rojhani E, et al. Spatial arrangement of testicular cells disrupted by transient scrotal hyperthermia and subsequent impairment of spermatogenesis. Andrologia 2020;52:e13664.

39. Pirani M, Novin MG, Abdollahifar MA, Piryaei A, Kuroshli Z, Mofarahe ZS. Protective effects of fisetin in the mice induced by long-term scrotal hyperthermia. Reprod Sci 2021;28:3123-36.

40. Delkhosh A, Shoorei H, Niazi V, Delashoub M, Gharamaleki MN, Ahani-Nahayati M, et al. Coenzyme Q10 ameliorates inflammation, oxidative stress, and testicular histopathology in rats exposed to heat stress. Hum Exp Toxicol 2021;40:3-15.

41. Sabry SA, Gomaa KA, Ibrahim HM. Histological and ultrastructural studies on the effect of haloperidol drug on testes of albino rats and the protective role of chitosan nanoparticles. J Biosci Appl Res 2017;3:150-60.

42. Kholodenko R, Kholodenko I, Sorokin V, Tolmazova A, Sazonova O, Buzdin A. Anti-apoptotic effect of retinoic acid on retinal progenitor cells mediated by a protein kinase A-dependent mechanism. Cell Res 2007;17:151-62.

43. Kang JB, Park DJ, Shah MA, Koh PO. Retinoic acid exerts neuroprotective effects against focal cerebral ischemia by preventing apoptotic cell death. Neurosci Lett 2021;757:135979.

44. Zhang MH, Shi ZD, Yu JC, Zhang YP, Wang LG, Qiu Y. Scrotal heat stress causes sperm chromatin damage and cysteinyl aspartate-spicific proteinases 3 changes in fertile men. J Assist Reprod Genet 2015;32:747-55.

45. Khafaga AF, El-Sayed YS. All-trans-retinoic acid ameliorates doxorubicin-induced cardiotoxicity: in vivo potential involvement of oxidative stress, inflammation, and apoptosis via caspase-3 and p53 down-expression. Naunyn Schmiedebergs Arch Pharmacol 2018;391:59-70.

46. Asfour MH, Salama AA, Mohsen AM. Fabrication of all-trans retinoic acid loaded chitosan/tripolyphosphate lipid hybrid nanoparticles as a novel oral delivery approach for management of diabetic nephropathy in rats. J Pharm Sci 2021;110:3208-20.

47. Rao J, Zhang C, Wang P, Lu L, Zhang F. All-trans retinoic acid alleviates hepatic ischemia/reperfusion injury by enhancing manganese superoxide dismutase in rats. Biol Pharm Bull 2010;33: 869-75.

48. Ahmed AZ, Satyam SM, Shetty P, D'Souza MR. Methyl gallate attenuates doxorubicin-induced cardiotoxicity in rats by suppressing oxidative stress. Scientifica (Cairo) 2021;2021:6694340.

49. Jha KN, Coleman AR, Wong L, Salicioni AM, Howcroft E, Johnson GR. Heat shock protein 90 functions to stabilize and activate the testis-specific serine/threonine kinases, a family of kinases essential for male fertility. J Biol Chem 2013;288:16308-20.

50. Pei Y, Wu Y, Qin Y. Effects of chronic heat stress on the expressions of heat shock proteins 60, 70, 90, A2, and HSC70 in the rabbit testis. Cell Stress Chaperones 2012;17:81-7.